

COMBINED  $^{17}\text{O}/^1\text{H}$  MAGNETIC RESONANCE MICROSCOPY IN PLANTS, ANIMALS AND MATERIALS:  
PRESENT STATUS AND POTENTIAL

G.D. MATEESCU,<sup>1</sup> G.M. YVARS,<sup>1</sup> D.I. PAZARA,<sup>1</sup> N.A. ALLDRIDGE,<sup>2</sup> J.C. LaMANNA,<sup>3</sup>  
W.D. LUST,<sup>4</sup> M. MATTINGLY,<sup>5</sup> W. KUHN,<sup>6</sup>  
Departments of Chemistry,<sup>1</sup> Biology,<sup>2</sup> Neurology,<sup>3</sup> and Neurosurgery<sup>4</sup>  
Case Western Reserve University, Cleveland, Ohio 44106 and  
Bruker Instruments, USA<sup>5</sup> and West Germany<sup>6</sup>

SUMMARY

$^{17}\text{O}$ -NMR imaging is shown to be a valuable alternative or complement to proton imaging. The properties of this nucleus, generally believed "unfavorable" for such applications, can in fact be turned into an advantage, and excellent images can be obtained. Moreover, the presence of  $^{17}\text{O}$  in  $\text{H}_2\text{O}$  at various levels of enrichment can drastically affect relative intensities in proton images. Thus, the  $^{17}\text{O}$  nucleus can constitute a useful, nontoxic, direct and indirect contrast agent in magnetic resonance imaging. After a brief presentation of the principles of magnetic resonance imaging, biomedical, biological and materials research applications are described in this paper. The prospects for using  $^{17}\text{O}$  in imaging and localized spectroscopy are discussed in the conclusion.

INTRODUCTION

Oxygen, the most abundant element on earth (and 4th in the universe), has three stable isotopes (16,17,18) and eleven, radioactive (12,13,14,15,19,20,21, 22,23,24 and 26). In spite of its essential role in life processes and general chemistry, its direct, noninvasive investigation remains to be achieved ( $^{15}\text{O}$ , used in respiration studies, is radioactive [positron emitter with 124 s half-life];  $^{18}\text{O}$  mass spectrometry is intrinsically destructive).

Our group has recently initiated studies (refs. 1-3) concerning the feasibility of  $^{17}\text{O}$  Magnetic Resonance Imaging (MRI). Based on highly sensitive proton detection, MRI is now being established as one of the most promising noninvasive investigation methods in medicine, biology and materials research.  $^{17}\text{O}$ , however, has been considered impractical as a direct imaging source due to the general belief that its properties are "unfavorable" for such studies. We present evidence that, in fact, these properties (low natural abundance, quadrupolar moment, fast relaxation) can be turned into advantage and excellent  $^{17}\text{O}$  imaging can be performed. Moreover, we show that, due to the coexistence and interaction of oxygen and hydrogen in  $\text{H}_2\text{O}$  (the principal source of imaging), combined  $^{17}\text{O}/^1\text{H}$  measurements greatly enhance the quality of image interpretation and open new research and diagnostic avenues.

## BASIC PRINCIPLES OF MAGNETIC RESONANCE IMAGING

Consider a water sample placed in the magnetic field  $B_0$  of a high resolution NMR spectrometer. The sample becomes magnetically polarized due to the preferential precession of the magnetic nuclei ( $^1\text{H}$ , spin  $I=1/2$ ;  $^2\text{H}$ ,  $I=1$ ;  $^{17}\text{O}$ ,  $I=5/2$ ) along  $B_0$ . The Boltzmann population equilibrium is reached exponentially with a time constant  $T_1$ , known as spin-lattice or longitudinal relaxation time because the magnetization builds up along  $B_0$  (conventionally taken on the z-axis). If a radiofrequency pulse covering the frequency range of one of the nuclei (e.g.,  $^1\text{H}$ ) is applied along the x-axis, the presence of the highly homogeneous field causes all water protons (found at any point in the transmitter/receiver coil volume) to resonate at a single frequency,  $\nu$  (or angular frequency  $\omega$ ), proportional to  $B_0$ :

$$\nu = (\gamma/2\pi)B_0 \quad \text{or} \quad \omega = \gamma B_0 \quad (\text{since } \omega = 2\pi\nu) \quad (1)$$

The proportionality factor,  $\gamma$ , is called the gyromagnetic ratio; it is a constant, characteristic of the measured nuclear spin, which determines the resonance frequency at a given field  $B_0$ . Once brought into the xy-plane by the rf pulse (which lasts for only a few  $\mu\text{s}$ ), the magnetization starts to decay exponentially due to spin-spin interactions which cause the spins to go out of phase; the variation of magnetization induces a current within the receiver coil (also placed perpendicular to the z-axis). The resulting signal, known as FID (free induction decay) is a time domain signal, a function which contains the resonant frequency information. The latter is retrieved by Fourier transformation in the form of a high resolution NMR spectrum (Figure 1a) with a single, sharp proton peak:

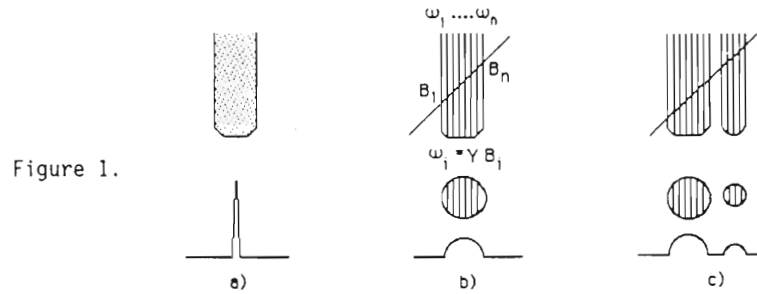
$$\begin{array}{ccc} f(t_d) & \text{----->} & F(\nu) \\ \text{(time domain)} & & \text{(frequency domain)} \end{array} \quad (2)$$

where  $t_d$  stands for "detection time" duration. The time constant of the xy-magnetization decay,  $T_2$ , is called spin-spin or transverse relaxation time (because the process takes place in a plane perpendicular to the z-axis). The line width is given by the full width at half-maximum (FWHM) of the peak:

$$\Delta\nu_{1/2} = 1/\pi T_2 \quad (\text{Hertz}) \quad (3)$$

If, however,  $B_0$  were not homogeneous, a broader line would be obtained. This suggests that in the presence of a linear field gradient there will be  $n$  successive regions in the sample resonating at  $n$  different frequencies increasing proportionally with the field gradient ( $n$  will depend on the resolution of the system). This means that one can now relate (encode) the resonance frequency of a nuclear spin with its physical position in the sample. The result of such an

experiment, as shown in Figure 1b, is a profile of the cylindrical water column along the gradient axis. It is now easy to imagine that, rotating the specimen



(or the field gradient) in a sufficient number of computer controlled positions, one can obtain the profile of an irregularly shaped sample by projection reconstruction. This was first discovered by Lauterbur (ref. 4) in 1973. Most of the imaging done today employs a different approach, namely two dimensional (2D) Fourier-transform techniques:

$$f(t_d, t[G_y]) \text{ -----> } F(v_x, v_y) \quad (4)$$

During  $t_d$  the x-gradient ( $G_x$ ) is turned on in order to ensure spatial frequency encoding (cf. Figure 1b). The "time variable" needed for transformation in the second dimension is achieved by successively incrementing the y-gradient ( $G_y$ ). This leads to a spatial phase encoding in the y-direction. In order to limit the image to a finite "slice" thickness, a "soft"  $90^\circ$  pulse is applied simultaneously with a z-gradient, at the beginning of the imaging sequence. The effect of this combination is described in Figure 2. An imaging sequence is

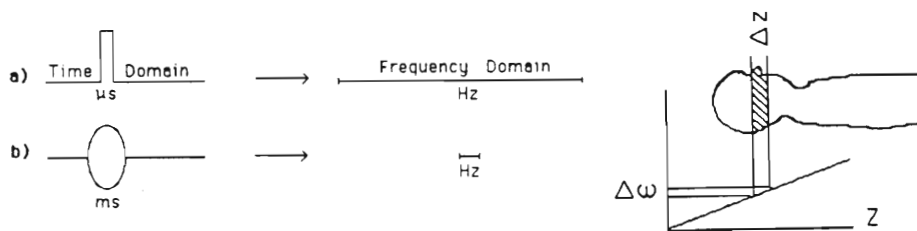
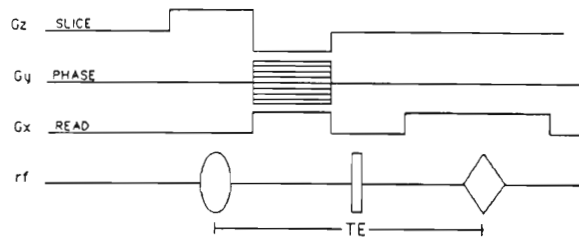


Figure 2. a) A short pulse duration covers a wide frequency domain; b) a longer pulse covers a narrow frequency domain; a soft pulse applied together with a z-gradient excites only the spins found in the slice corresponding to  $\Delta\omega$ .

presented in Figure 3. The application of positive and negative gradients is needed to refocus the spins just before the detection time. The rf pulses,

soft 90 and hard 180°, produce a spin-echo signal which is spatially encoded by the "read" gradient,  $G_x$ . Further details can be found in two reviews (ref. 5) and references cited therein.

Figure 3. A gradient refocussing spin-echo imaging sequence. TE = time of echo.



Since the measurement is always made some time after pulse excitation and, in order to build sufficient signal-to-noise it is necessary to accumulate the signals of repetitive scans, the image intensity depends on both the  $T_2$  and  $T_1$  properties of the specimen. This makes it possible to obtain  $T_1$  or  $T_2$  weighted images by selecting an imaging sequence with appropriately ordered and timed rf and gradient pulses. Due to the fact that relaxation times are intrinsically related to molecular motion, it is possible, for example, to distinguish various kinds of normal and pathological tissues, according to the degree of freedom of their associated water. Internal motion in polymers and polymer blends can be investigated. Liquid flow and penetration at interfaces can also be studied.

#### MAGNETIC RESONANCE PROPERTIES OF OXYGEN-17 AND THEIR MANIFESTATION IN MRI

The great majority of papers or reviews concerning  $^{17}\text{O}$  NMR studies emphasize the fact that the magnetic properties of  $^{17}\text{O}$  are "unfavorable" for nuclear magnetic resonance studies. A comparison of these properties to those of proton seems to support this view, particularly when imaging experiments are considered (see Table 1, which also contains data for other "rare" nuclei). However, we have recently demonstrated that  $^{17}\text{O}$  MRI is feasible; moreover, it has some distinct advantages. Thus, because of the very low natural abundance of  $^{17}\text{O}$ , an isotopic enrichment of 37% would enhance detection by a factor of 1,000 with a reduction of the measurement time by  $10^6$ . Furthermore, the fast quadrupolar relaxation allows pulsing rates at least 20 times faster without signal loss. These conditions compensate for most of the losses due to quadrupolar broadening. The latter can also be considered as an asset since it confers the  $^{17}\text{O}$  nucleus short range sensitivity to the surrounding electronic structure. The strong line width dependence on the correlation time allows better distinction of the "free" and "bound" states of water (the principal signal source for

imaging). Moreover,  $^{17}\text{O}$  is the sole isotope which can yield direct relaxation information on water interactions with its environment because it is not affected by cross-relaxation as is  $^1\text{H}$ , or exchange processes, as are  $^1\text{H}$  and  $^2\text{H}$  (see refs. 6,7 and literature cited therein).

TABLE 1  
Magnetic and NMR properties of  $^1\text{H}$ ,  $^2\text{H}$ ,  $^{13}\text{C}$ ,  $^{15}\text{N}$  and  $^{17}\text{O}$  nuclei

Property	$^1\text{H}$	$^2\text{H}$	$^{13}\text{C}$	$^{15}\text{N}$	$^{17}\text{O}$
Spin (I)	1/2	1	1/2	1/2	5/2
Magnetic moment <sup>a</sup>	2.79268	0.857387	0.702199	0.28298	-1.893997
Gyromagnetic ratio <sup>b</sup>	4257.6	653.6	1070.5	431.4	577.2
NMR frequency at 9.395 Tesla <sup>c</sup>	400	61.402	100.577	40.531	54.227
Chemical shift range <sup>d</sup>	20	20	300	600	1500
Quadrupole moment <sup>e</sup>	-	0.00273	-	-	-0.026
Natural abundance <sup>f</sup>	99.985	0.015	1.108	0.365	0.037
Relative sensitivity <sup>g</sup>	1.00	$9.65 \times 10^{-3}$	$1.59 \times 10^{-2}$	$1.04 \times 10^{-3}$	$2.91 \times 10^{-2}$
Receptivity <sup>h</sup>	1.00	$1.45 \times 10^{-6}$	$1.76 \times 10^{-4}$	$3.85 \times 10^{-6}$	$1.08 \times 10^{-5}$

a) nuclear magneton units; b) Hz/Gauss; c) MHz; d) ppm, approximate range; e) electron  $\text{cm}^2$ ; f) %; g) at constant field for equal number of nuclei; h) relative sensitivity multiplied by natural abundance

#### EXPERIMENTAL METHODS

The proton and  $^{17}\text{O}$  images were taken with a Bruker MSL-400 NMR microscope operating at 400.13 and 54.24 MHz, respectively. The microimaging accessory, operated from the console of the high resolution spectrometer, consists of: an image graphics display processor; a high-resolution B/W monitor; x,y,z-gradient amplifiers; a gradient preemphasis unit and gradient wave form memories (for compensation of Eddy currents); selective excitation unit containing rf wave form memory (for various soft pulse shapes); an rf pulse amplitude modulator and linear amplifier; a probe with integral gradient coil assembly; imaging software.

For a given gradient strength,  $g$ , the resolution is limited by the line-width:  $\Delta x = 1/\pi T_2 \gamma g$ . Thus, for a 10  $\mu\text{m}$  pixel (picture element) resolution in the xy-plane, at a proton relaxation  $T_2 = 10$  ms, we would need 7.5 Gauss/cm. Our system allows  $g \sim 100$  Gauss/cm. This is particularly useful for  $^{17}\text{O}$  imaging since, in order to achieve reasonable resolution one needs more than seven times gradient strength (because  $\gamma_{\text{H}}/\gamma_{\text{O}} = 7.37$ ). Of course, the resolution also depends on signal-to-noise (the smaller the voxel [volume element] to be imaged, the larger S/N needed) which, in full relaxation conditions, is

mainly determined by proton density and instrumental factors. The inhomogeneous broadening or spread of chemical shifts add to resolution impairment. The slice thickness (ST) is given by:  $\Delta z = \Delta f / \gamma g_z$ , where  $\Delta f$  is the frequency bandwidth of the soft (slice selective) pulse.

Oxygen-17 enriched water (40-51 atom %) was purchased from Monsanto's Mound Laboratory, Miamisburg, Ohio, operated under contract for the U.S. Atomic Energy Commission. Animal anesthesia was performed with chloral hydrate.

## RESULTS AND DISCUSSION

### Comparison between $^1\text{H}$ and $^{17}\text{O}$ imaging

The exceptional contrast power of  $^{17}\text{O}$  as a direct imaging source is demonstrated with a phantom consisting of seven capillaries: four were filled with natural abundance water and three, with  $\text{H}_2^{17}\text{O}$  (5 atom %). The ensemble was immersed in an 8mm OD glass tube containing  $^{17}\text{O}$  enriched water (5 atom %). Figure 4a represents the proton image of a transverse slice (0.5 mm thick) taken in 4.3 min. No distinction can be made between natural abundance and  $^{17}\text{O}$

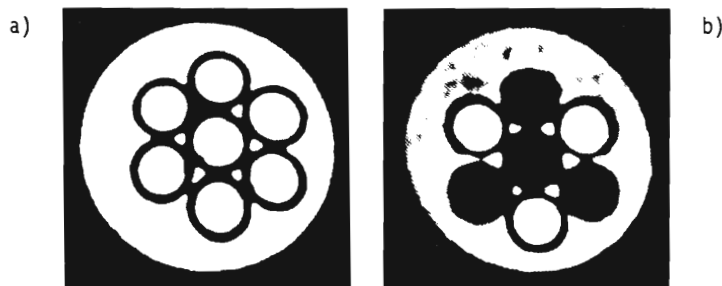


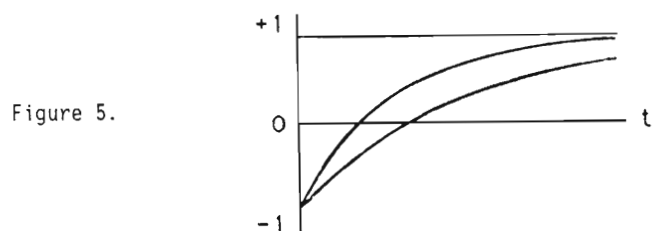
Figure 4.

enriched water. Figure 4b shows the  $^{17}\text{O}$  image of the same phantom (2 mm slice) taken in 6.3 min. It is seen that there is a practically infinite contrast between the bright image of the  $^{17}\text{O}$  enriched water and the completely dark image of the natural abundance water.

### Oxygen-17 as contrast agent in $^1\text{H}$ imaging

As mentioned above, the nature and timing of an imaging sequence (order and interval of gradient and rf pulses) may enhance or diminish the contrast between regions of the specimen having different  $T_1$  and/or  $T_2$  values. For example, if a  $180^\circ$  pulse is placed in front of the sequence shown in Figure 3, the spin population is inverted in the entire sample. Immediately after the pulse the longitudinal relaxation begins to restore the z-population to its initial value (95% of which is reached after  $\sim 3 \times T_1$ ). Varying the time at

which the observe ( $90^\circ$ ) pulse is applied will result in signals ranging in intensity from -1 to +1. As seen in Figure 5, employing this sequence, called inversion recovery (IR), one can completely eliminate the signal from one or the other of two components with different  $T_1$ 's by choosing the measurement time at the appropriate zero-crossing point ( $t_{zc} = 0.693T_1$ ). Of course, in our



imaging sequence (cf. Figure 3) the echo time (TE) is also important because it will affect the signal intensity in function of  $T_2$ .

It results that varying the recovery time and or the repetition time (TR) of the sequence, one can enhance or diminish the intensity of a component in an image if its relaxation properties are different from those of the other components.

Previous studies have shown that the presence of increasing amounts of  $^{17}O$  in water affect both the  $T_1$  (refs. 1-3) and  $T_2$  (ref. 8) of proton. We demonstrate in Figure 6 that a wide variety of contrasts can be obtained by varying

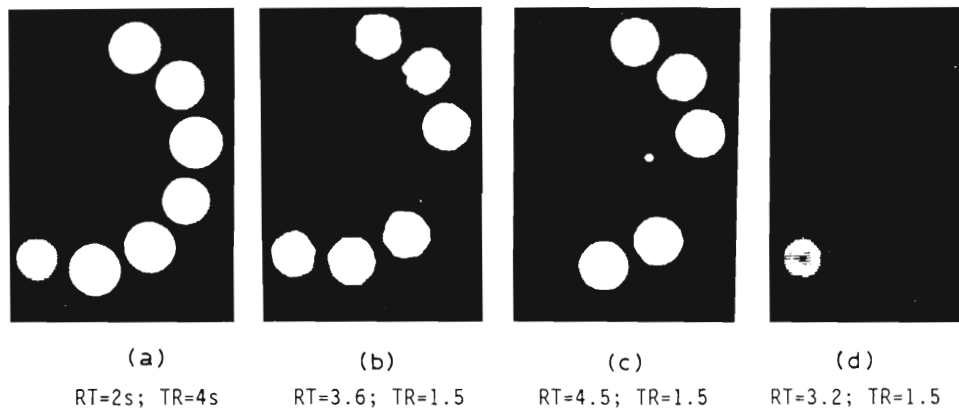


Figure 6. Proton images of 7 capillaries filled with natural abundance (NA) and  $^{17}O$  enriched (atom %) water, as follows (clockwise, from top): NA - 10% - NA - 20% - NA - NA - 40%. Recovery and repetition times are indicated for each run.

the magnetization recovery time (RT) and TR. An even larger contrast "palette" should be obtained by also including the variation of TE.

Whole body  $^{17}\text{O}/^1\text{H}$  imaging of small animals.

Figure 7 represents the  $^{17}\text{O}$  image (a 2.5 mm slice at the stomach level) of a 20g mouse sacrificed 40 minutes after i.p. injection of 0.5 ml  $\text{H}_2^{17}\text{O}$  (40 atom %) i.e., 10 g/kg. The image was obtained in 12.8 minutes. A control run on an animal injected (i.p.) 0.5ml saline solution made with natural abundance water yielded a completely dark "image". This experiment demonstrates the outstanding



Figure 7.

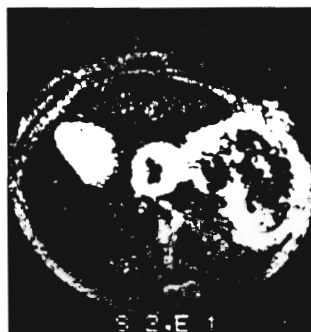


Figure 8.

potential of  $^{17}\text{O}$  as a contrast agent in MRI.

Moreover, the  $^{17}\text{O}$  induced contrast enhancement demonstrated by us in the previous section has been also observed in the proton image of a 9g nude mouse after having been given 250  $\mu\text{l}$  overnight,  $\text{H}_2^{17}\text{O}$  (50 atom %) in food and 130  $\mu\text{l}$  just prior to observation. It is seen in Figure 8 (slice thickness = .5 mm) that the stomach and esophagus walls display a dramatic contrast due to  $^{17}\text{O}$  relaxation effects.

Studies of water uptake and distribution in plants.

Preliminary studies with a plant stem suggest that the combined  $^{17}\text{O}/^1\text{H}$  imaging will be a valuable method of in vivo investigation of plant physiology, metabolism, and pathology. The sketch in the upper left corner of Figure 9 depicts the experimental arrangement and the position of the axial slices shown in Figures 9a-f. An  $^{17}\text{O}$  image taken immediately after immersion in  $\text{H}_2^{17}\text{O}$  (25 atom %) revealed the huge contrast between the enriched water surrounding the stem and the natural abundance water contained within the stem. Five minutes after immersion, the  $\text{H}_2^{17}\text{O}$  ascended to the level shown in the sketch for Figure 9b. In order to avoid the flooding of the image with the signal from the enriched water, slices c,d,e and f were taken above the level of the  $\text{H}_2^{17}\text{O}$  at

20, 40, 60 and 300 min after immersion. The progressive intake of the  $^{17}\text{O}$  water by the plant can be clearly followed. The  $^{17}\text{O}$  signal is extremely strong. This means that thinner slices at higher resolution are attainable.

As with experiments on animals described above, strong  $^{17}\text{O}$  induced contrast has also been observed in proton images of plants.

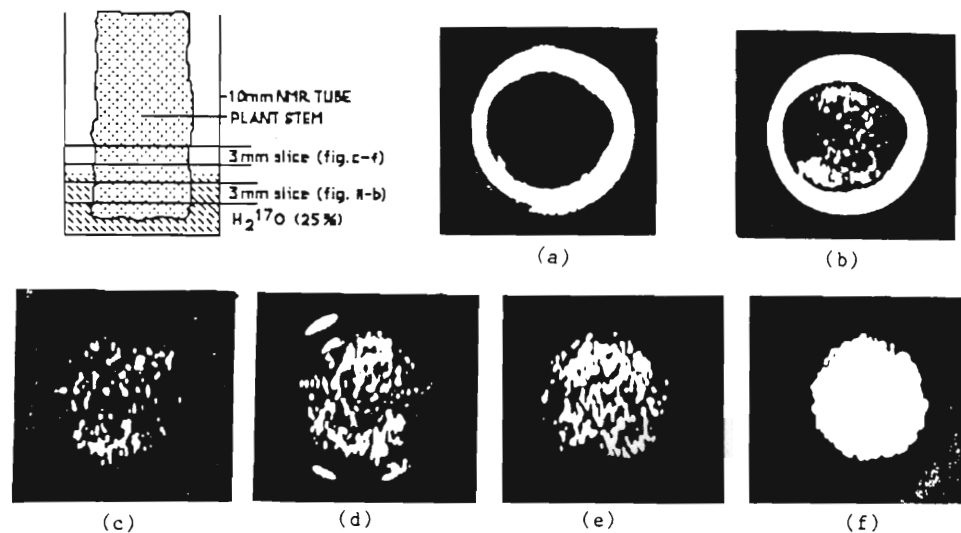


Figure 9.

## CONCLUSIONS

### Present status of the use of O-17 labelled compounds in MRI

During the past year, the feasibility of  $^{17}\text{O}$  MRI has been fully demonstrated (refs. 1-3). With  $^{17}\text{O}$  enrichments of water to <5%, strong intensity images have been obtained. It has been shown that the total lack of background signal (due to the very low natural abundance of  $^{17}\text{O}$ ) affords highly contrasted images both in live organisms and in materials.

The second outstanding result of these experiments is the observation of dramatic and widely varied contrast induced by  $^{17}\text{O}$  in  $^1\text{H}$  images. Work in progress in our laboratory includes: a systematic *in vivo* study of distribution and time of residence of exogenous  $\text{H}_2^{17}\text{O}$  in small laboratory animals with emphasis on the nervous system, particularly the brain; preliminary experiments with  $\text{P}^{17}\text{O}_4^{3-}$ ,  $\text{HC}^{17}\text{O}_3^-$  and  $\text{S}^{17}\text{O}_4^{2-}$ ; *in vivo* plant anatomy and physiology; materials research (moisture ingress and diffusion in polymers and composites).

### Prospects

The most important application we foresee for  $^{17}\text{O}$  and combined  $^{17}\text{O}/^1\text{H}$  imaging and localized spectroscopy is in biomedical research and radiological diagnostic (our experiments agree with those of other laboratories [ref. 8 and literature cited therein] that  $\text{H}_2^{17}\text{O}$  is not toxic). It is possible that  $^{17}\text{O}$

will help replace today's invasive coronary angiography with a simple contrast agent MRI. Volume selected spectroscopy will facilitate the noninvasive tracing of endogenous (metabolic) water. Some of the most important biological molecules, glucose, vitamin C, etc., have a high oxygen content; they are metabolized into H<sub>2</sub>O or small molecules which have adequate correlation times for <sup>17</sup>O imaging. Respiration studies with labelled O<sub>2</sub> and CO<sub>2</sub> are deemed possible. Food and agricultural research will benefit from in vivo studies of seeds and seedlings. <sup>17</sup>O imaging will complement <sup>1</sup>H imaging in materials research for unequivocal detection of moisture penetration and diffusion in polymers, composites and interfaces when intrinsic and exogenous proton signals overlap. The need to image components with shorter relaxation times will cause a comeback of the projection reconstruction technique.

ACKNOWLEDGMENTS. We thank A.Valeriu for valuable technical assistance and helpful discussions. M. Jakupca, NSF summer undergraduate fellow, and K. McCracken made useful contributions to this work. These studies were conducted in the Major Analytical Instruments Facility of the Department of Chemistry. Grants from NSF, NIH, CWRU and the Ohio Board of Regents are gratefully acknowledged.

#### REFERENCES

- 1 a) G.D. Mateescu, G.M. Benedikt and M.P. Kelly, New Dimensions in O-17 Nuclear Magnetic Resonance Spectroscopy, in W.P. Duncan & A.B. Susan (Eds.), Proc. Int. Symp. Synt. Appl. Isotop. Labeled. Cpd., Kansas City, MO, USA, 6-11 June 1982, Elsevier, Amsterdam, 1983, pp.483-484.  
b) G.D. Mateescu, G.M. Yvars, D.I. Pazara and N.A. Alldridge, O-17/Proton NMR Microscopy, ENC (Experimental NMR Conference), Rochester, N.Y., April 1988, p. 189.  
c) G.D. Mateescu, G.M. Yvars and T. Dular, Water, Ions, and O-17 Magnetic Resonance Imaging, in: V. Vasilescu, (Ed), Proc. 4th Int. Conf. on Water and Ions in Biol. Systems, Bucharest, May 24-28, 1987, Birkhauser, Boston, 1988.
- 2 a) G.D. Mateescu, G.Yvars and T.Dular, Oxygen-17 Magnetic Resonance Imaging, Proc. Soc. Mag. Res. Med., (1987) 929.  
b) G.D. Mateescu, G.M. Yvars, D. Pazara and N.A. Alldridge, NMR Microscopy, Applications in Agricultural and Food Chemistry, ACS Symposium Series, 1988, in preparation.
- 3 G.D. Mateescu, G.M. Yvars, D. Pazara, J.C. LaManna, W.D. Lust, K. McCracken, M. Mattingly, and W. Kuhn, Oxygen-17: A Physiological, Biochemical and Anatomical MRI Contrast Agent, Proc. Soc. Mag. Res. Med, San Francisco, August 22-26, 1988.
- 4 P. Lauterbur, Image Formation by Induced Local Interactions: Examples Employing Nuclear Magnetic Resonance, Nature 242 (1973) 190-1.
- 5 a) E.R. Andrew, NMR Imaging, Accts. Chem. Res., 16 (1983) 114.  
b) S.L. Smith, NMR Imaging, Analytical Chemistry, 57 (1985) 595A.
- 6 L. Piculell and B. Halle, Water Spin Relaxation in Colloidal Systems, Part 2. O-17 and H-2 Relaxation in Protein Solutions, J. Chem. Soc., Faraday Trans., 1, 82 (1986) 401-414.
- 7 M.P. Bozonnet-Frenot, J.P. Marchal and D. Canet, Water O-17 and H-2 Longitudinal Nuclear Magnetic Relaxation in Aqueous Surfactant Solutions, J. Phys. Chem., 91 (1987) 89-94.
- 8 A.L. Hopkins and R.G. Barr, Oxygen-17 Compounds as Potential NMR T<sub>2</sub> Contrast Agents: Enrichment Effects of H<sub>2</sub><sup>17</sup>O on Protein Solutions and Living Tissues, Magnetic Resonance in Medicine, 4 (1987) 399-403.